RNA (2001), *7*:1213–1226. Cambridge University Press. Printed in the USA.

DOI: 10.1017.S1355838201010433

IRES interaction with translation initiation factors: Functional characterization of novel RNA contacts with eIF3, eIF4B, and eIF4GII

SONIA LÓPEZ DE QUINTO, ESTHER LAFUENTE, and ENCARNACIÓN MARTÍNEZ-SALAS
Centro de Biología Molecular Severo Ochoa, CSIC-UAM, Cantoblanco, 28049 Madrid, Spain

ABSTRACT

Translation initiation promoted by picornavirus internal ribosome entry site (IRES) elements is dependent on the association of specific IRES sequences to the initiation factor eIF4G. However the RNA determinants interacting with other components of the translational machinery are still unknown. In this study, we have identified novel RNA–protein interactions between the foot-and-mouth disease virus (FMDV) IRES and three translation initiation factors. A doublet of 116/110 kDa that crosslinked to the FMDV IRES is a component of eIF3. We show here that domain 5 holds the preferential binding site for eIF3, although this complex initiation factor can establish multiple contacts with the IRES structure. We have also identified the phylogenetically conserved hairpin of domain 5 as the RNA motif responsible for eIF4B interaction. Mutation of this stem-loop structure abrogated eIF4B, but not eIF3, binding to the IRES. Remarkably, IRES mutants severely affected in their interaction with eIF4B showed a mild reduction in IRES activity when tested in the context of a bicistronic expression vector in transfected cells. Finally, we provide evidence of the interaction of eIF4GII with FMDV IRES, the RNA determinants for this interaction being shared with its functional homolog eIF4GI. The FMDV Lb protease generated a C-terminal fragment of eIF4GII that binds to the IRES as efficiently as the intact protein. Competition experiments showed that titration of eIF4B or p110/116 interaction with the FMDV IRES required a large excess of competitor relative to eIF4G, strongly suggesting that eIF4G-IRES interaction is a limiting factor to titrate the IRES. Comparative analysis of the activity of IRES mutants affected in domains 4 and 5 regarding their pattern of RNA–protein complex formation demonstrates that while binding of eIF4B with the FMDV IRES is dispensable, interaction of eIF4G is a central feature of the activity of this element.

Keywords: foot-and-mouth disease virus (FMDV); IRES; RNA-protein interaction; translation initiation factors (eIF)

INTRODUCTION

Internal translation initiation is mediated by a *cis*-acting element, known as the internal ribosome entry site (IRES), that positions the translational machinery near an internal initiator codon in the mRNA. IRES elements were first described in picornavirus RNAs (Jang et al., 1988; Pelletier & Sonenberg, 1988). They are also present in other viral RNAs and in a growing number of cellular mRNAs (Carter et al., 2000). The RNA that conforms the IRES plays an active role in the mechanism of internal initiation, the overall RNA structure being a crucial determinant for the interaction of specific IRES sequences with the translation machinery (Belsham & Jackson, 2000; Martínez-Salas et al., 2001).

During the last years, it has become increasingly clear that different IRESs use distinct strategies to interact with the translational machinery (Pestova et al., 1998b; Wilson et al., 2000). Remarkably, eukaryotic translation initiation factors (eIF) play an essential role in picornavirus IRES-dependent initiation (Kolupaeva et al., 1998; López de Quinto & Martínez-Salas, 2000; Pilipenko et al., 2000). The encephalomyocarditis virus (EMCV) and foot-and-mouth disease virus (FMDV) IRESs were described to depend on eIF4A, eIF4G, eIF2, and eIF3 for 48S complex formation in vitro (Pestova et al., 1996; Kolupaeva et al., 1998; Pilipenko et al., 2000). In contrast to picornavirus IRESs, hepatitis C virus (HCV) and classical swine fever virus (CSFV) IRESs required

Reprint requests to: Encarnación Martínez-Salas, Centro de Biología Molecular Severo Ochoa, CSIC-UAM, Cantoblanco, 28049 Madrid, Spain; e-mail: emartinez@cbm.uam.es.

only eIF2•GTP•Met-tRNA, eIF3, and 40S subunits to assemble the 48S initiation complex (Pestova et al., 1998b).

The mammalian eIF3 contains 11 subunits of which p170, p116 and p110, p66, p47, and p44 have RNA-binding capacity (Nygard & Westermann, 1982; Asano et al., 1997; Block et al., 1998; Buratti et al., 1998; Sizova et al., 1998). eIF3 binds to the small ribosomal subunit, stabilizes the binding of the eIF2•GTP•Met-tRNA ternary complex to the 40S subunit, and promotes dissociation of 80S ribosomes (Hershey & Merrick, 2000). Binding of eIF3 to the apical region of domain III of both HCV and CSFV IRESs has been described (Buratti et al., 1998; Sizova et al., 1998). To date, there is no data concerning the interaction of eIF3 complex with other IRESs.

eIF4B is an 80-kDa RNA-binding protein (Meyer et al., 1982; Milburn et al., 1990b; Méthot et al., 1996a) that stimulates the ATPase and helicase activities of eIF4A (Rozen et al., 1990) and strengthens the mRNA–rRNA–tRNA interaction at the initiation codon (Altmann et al., 1995). eIF4B stimulates slightly 48S complex formation in vitro on EMCV IRES and β-globin mRNA (Pestova et al., 1996, 1998a) and binds to sequences within the 3′ end of the FMDV and EMCV IRES (Meyer et al., 1995; Kolupaeva et al., 1998; López de Quinto & Martínez-Salas, 2000). Despite its strong RNA-binding efficiency, the biological relevance of eIF4B-RNA interaction in IRES-dependent initiation awaits elucidation.

eIF4G is a component of eIF4F, together with eIF4E and eIF4A. It serves as an adaptor that allows circularization of capped, polyadenylated mRNA (Tarun & Sachs, 1996; Preiss & Hentze, 1999). Two eIF4G functional homologs exist, eIF4GI and eIF4GII (Gradi et al., 1998a). During polio and rhinovirus infection, the protease 2A cleaves both forms of eIF4G, inducing the inactivation of cap-dependent translation (Gradi et al., 1998b; Svitkin et al., 1999). The Lb protease of FMDV is able to process eIF4GI (Kirchweger et al., 1994; Lamphear et al., 1995) but there are still no studies of eIF4GII integrity in FMDV-infected cells. The carboxy-terminal end of eIF4GI generated by the Lb protease binds to the FMDV IRES as efficiently as the unprocessed protein (López de Quinto & Martínez-Salas, 2000). This eIF4GI fragment contains the binding sites for eIF3 and eIF4A (Gingras et al., 1999) and accordingly, eIF4A stimulates binding of the central part of eIF4GI to the EMCV and FMDV IRESs (Lomakin et al., 2000; Pilipenko et al., 2000). Although it has been recently shown that the central region of eIF4GII allows EMCV IRES-dependent 48S complex formation in vitro (Marcotrigiano et al., 2001), little is known about the RNA determinants required for eIF4G–IRES interaction that could account for a preferential mRNA binding of eIF4GI versus eIF4GII.

The FMDV IRES is predicted to fold into five domains, all of which contribute to the activity of the element (Martínez-Salas et al., 2001). To study the RNA determinants responsible for the interaction between the FMDV IRES and the components of the translation machinery, we compared the RNA–protein interaction pattern of the IRES with that of the separated domains. The 3′ region of the IRES presented a similar pattern to that observed for the whole IRES (López de Quinto & Martínez-Salas, 2000) with the exception of the polypyrimidine tract binding protein (PTB) whose major binding site resides in domain 2 (Luz & Beck, 1991). The RNA sequences conforming domains 4–5 are responsible for the interaction with eIF4GI and eIF4B, as well as with a 120-kDa protein. With the exception of eIF4GI, for which a direct correlation between binding and in vivo IRES activity has been demonstrated (López de Quinto & Martínez-Salas, 2000), the requirement of eIF4B interaction for internal initiation of translation is not clear, and neither is the identity of p120 known.

In this report, we have identified a component of eIF3 crosslinked to the FMDV IRES. We have mapped the eIF4B-binding site in domain 5 of this IRES. Additionally, we present experimental evidence of the direct binding of the eIF4GII protein with the FMDV IRES. Furthermore, we have studied the biological relevance of these interactions analyzing the activity of IRES mutants in regard to their pattern of RNA–protein interactions. These results led us to demonstrate that although eIF4B interaction with the FMDV IRES is dispensable, interaction of eIF4G is a central feature of the activity of this element.

RESULTS

Fine mapping of the FMDV IRES sequences required for RNA–protein interactions

We have shown previously that the 3′ region of the FMDV IRES is essential to establish functional interactions with eIF4GI (López de Quinto & Martínez-Salas, 2000). To define IRES sequence determinants for functional interactions with other components of the translational machinery, we have analyzed in detail the interaction pattern of subdomains conforming the 3′ region of the FMDV IRES with cellular proteins. To this end, we generated a series of constructs encompassing domains 4 and 5 or combinations of their structural motifs (Fig. 1A,B). All constructs were designed to maintain the predicted secondary structure of each functional domain in the full-length IRES.

Transcripts containing the structural motifs of interest were used in UV-crosslinking assays with S10 extracts prepared from BHK-21 cells in which FMDV replicates efficiently, or HeLa cells that support efficient IRES activity. When transcript d4-5 was used as probe, crosslinking of proteins with apparent molecular masses of 220, 116, and 80 kDa was observed (Fig. 1C), consis-

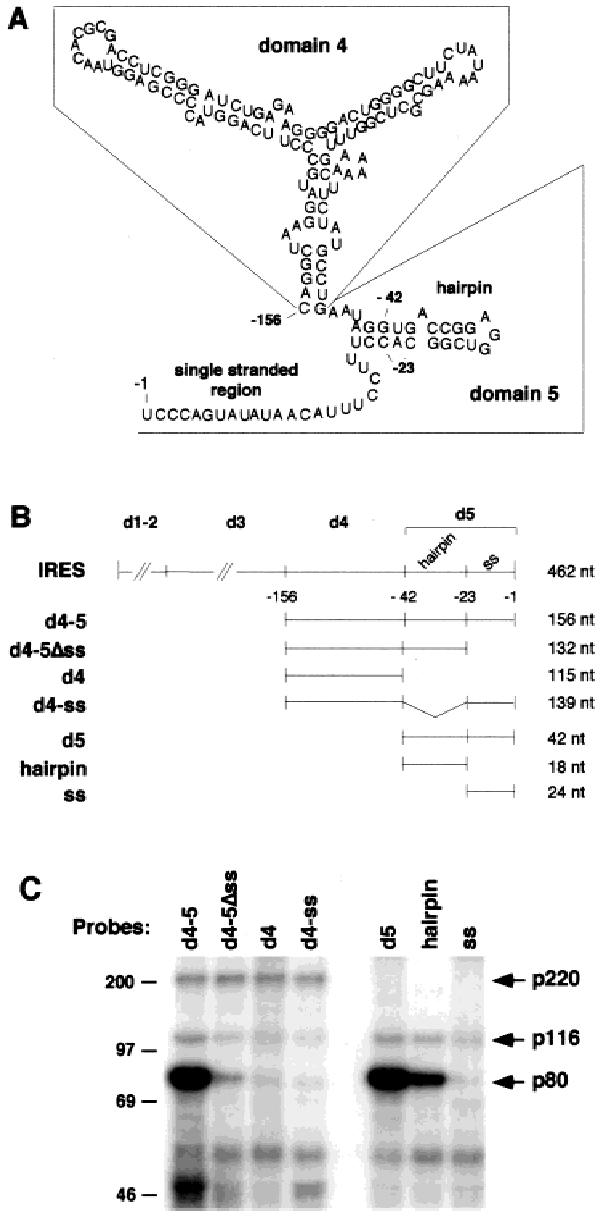

FIGURE 1. Analysis of the interaction pattern of the 3′ end of FMDV IRES with cellular proteins. **A:** Predicted secondary structure of the 3′ end of FMDV IRES, including domains 4 and 5. Numbers indicate the residue flanking the domains studied, considering +1 position the A of the first functional AUG codon in the FMDV RNA (López de Quinto & Martínez-Salas, 1999). **B:** Schematic representation of the IRES subdomains used as probes in RNA–protein interaction studies. Next to each transcript the nucleotide length of the viral RNA is specified. **C:** The radiolabeled transcripts indicated on top of each lane (0.04 pmol) were used in UV-crosslinking assays with native proteins present in a S10 BHK-21 cell extract. Following RNase A treatment, proteins were fractionated in 8% SDS-PAGE. The apparent molecular mass of the crosslinked polypeptides is indicated on the right, and the migrating positions of molecular mass markers on the left.

tent with previous studies of this IRES. However, the crosslinked protein previously named p120 showed an apparent molecular mass ranging from 110 to 116 kDa. Thus, this protein will be referred as p116 in this study.

Crosslinking of p220 was only detected using probes that contained domain 4, whereas no interaction was observed in RNAs encompassing the hairpin and/or the single-stranded region of domain 5 (Fig. 1C). These observations support the notion that the binding site of p220, previously identified as eIF4GI (López de Quinto & Martínez-Salas, 2000) is restricted to sequences within domain 4 of FMDV IRES. In contrast, p116 crosslinking was observed with all the probes that contained the 3′ end of the IRES (Fig. 1C). Crosslinking of p116 was more efficient in transcripts including the hairpin of domain 5, suggesting that this structure holds a preferential binding site for this protein. However, we can detect p116 crosslinked to domain 4 as well as to the single-stranded region of domain 5, although with lower efficiency than to the hairpin probe (Fig. 1C).

Efficient IRES interaction with p80, previously identified as eIF4B (Meyer et al., 1995), was seen only with probes that include the stem-loop of domain 5 (Fig. 1C). Interestingly, the hairpin probe crosslinked p80 with high efficiency, indicating that the stem-loop of domain 5 is necessary and sufficient to ensure eIF4B binding to FMDV IRES. In fact, the sequence of the ss probe (24 nt) did not present determinants necessary for p80 recognition as this transcript per se was not able to crosslink p80 (Fig. 1C). However, the single-stranded region apparently stabilized eIF4B-IRES interaction. Comparison of the probes containing or not containing this sequence revealed a decrease in p80 crosslinking when deletion of the single-stranded region was performed (7% of p80 crosslinking in d4-5Δss probe relative to d4-5; 24% of p80 crosslinking in the hairpin probe relative to d5).

The pattern of p116 crosslinking differed in its apparent lack of specificity from that of p220 and p80. Because no common sequences or structural motifs were detected in probes crosslinked to p116, we reexamined p116 binding to the separated FMDV IRES domains. A weak crosslinking of p116 to domains 1–2 and 3 (17% and 25% of binding relative to domain 5, respectively) was observed in overexposed films (Fig. 2, left panel). This result suggested the existence of multiple contacts of p116 in the FMDV IRES.

The RNA–protein interaction pattern displayed by subdomains of the FMDV IRES showed that the 44 nt that constitutes domain 5 contains the RNA determinants to crosslink a large subset of proteins that binds to the full-length IRES (Fig. 2). The exceptions to this pattern are domain 3, which interacts with a doublet of about 45 kDa (Fig. 2, right panel), and domain 4, interacting with p220. On the other hand, some weak binding proteins such as p170 were not detected in the complete IRES. Instead, a protein of 150 kDa crosslinked weakly to the IRES or d4-5 probes (Fig. 2). Differences in the intensity of the crosslinked products of up to 100-fold can be detected between the strongest crosslinked pro-

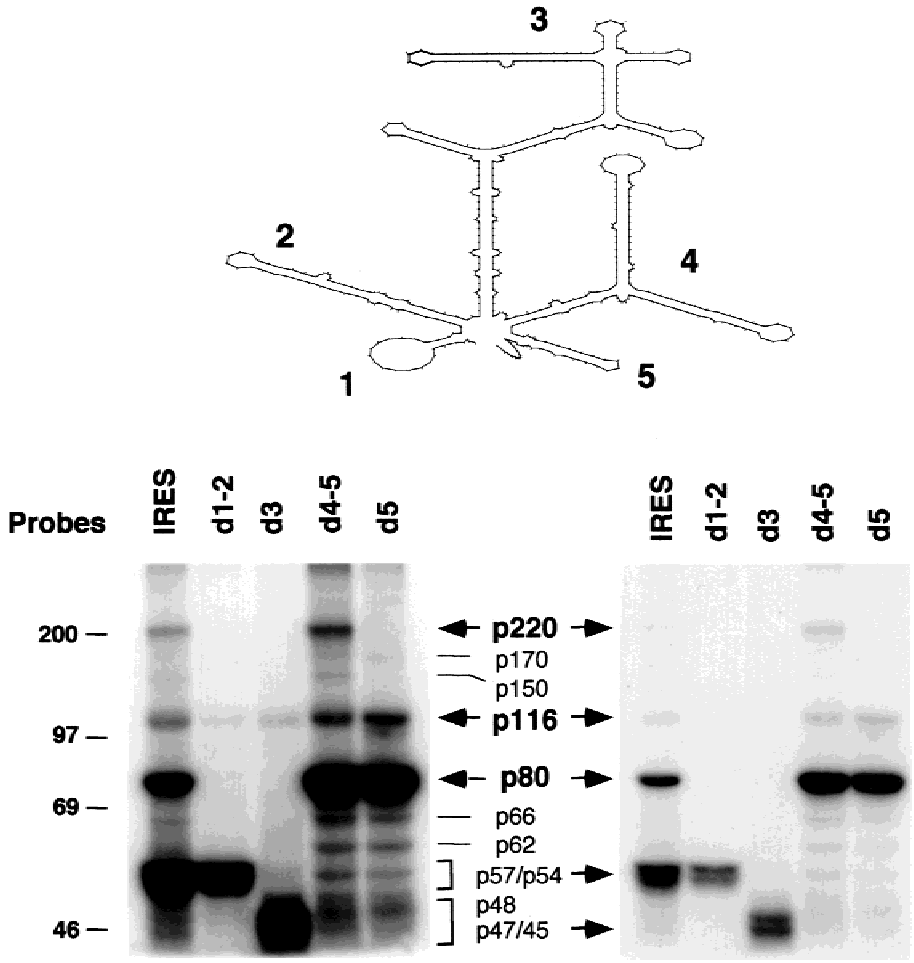

FIGURE 2. RNA–protein crosslink pattern with domains of the FMDV IRES. On the left panel, an overexposed film shows the UV-crosslinked proteins to the separated domains of the FMDV IRES, resolved in 8% SDS-PAGE. A short exposure of the same dry gel is shown on the right panel. The protein crosslinked to d1-2 is a doublet of 54 and 57 kDa (PTB); the protein that crosslinked to d3 is also a doublet of 45 and 47 kDa. Constructs d1-2 and d3 have been described (Ramos & Martínez-Salas, 1999). The full-length IRES, with its domains numbered 1 to 5, is shown on the top.

tein (p80 with domain 5) compared to the interaction of p116 with domain 1–2.

The 116 kDa protein that interacts with FMDV IRES is a component of eIF3

The nature of p116 interacting with the FMDV IRES was unknown. Interestingly the apparent molecular mass of some of the proteins that crosslinked to domain 5 (p170, p116, p66, p46 in Fig. 2) were coincident with several eIF3 polypeptides with RNA-binding capacity. To test the possibility that p116 could be a component of the eIF3 complex, we first compared the RNA–protein interaction pattern of the 3′ end region of FMDV IRES to that of HCV IRES in our UV-crosslinking assay. Thus, d4-5 and d5 were used as probes in parallel to HCV RNAs corresponding to the whole IRES and to domain III, as this structure has been shown to interact with eIF3 (Buratti et al., 1998; Sizova et al., 1998).

Regardless of the source of protein assayed, BHK-21 or a HeLa cell extract, similar polypeptides were crosslinked to d4-5 and d5 of FMDV IRES (Fig. 3). Remarkably, when HCV transcripts were used as probes with BHK-21 extracts, the interaction of p116 was observed. In the case of HeLa cell extracts, a p170 crosslinked efficiently to HCV RNAs was detected, in addition to p116. These results indicate that the RNA–protein interaction pattern of HCV IRES could vary depending on the protein source used for the UV-crosslinking assay.

Interestingly, p116 interacting with FMDV RNAs comigrated with that crosslinked to HCV probes (Fig. 3) suggesting that it could correspond to the same protein. Identification of p116 was performed by immunocharacterization of the proteins crosslinked to the FMDV IRES in parallel to those interacting with HCV IRES. It should be noted that when proteins were resolved in a 7% SDS-PAGE, a broad band corresponding to p116 was detected, ranging from 107 to 120 kDa (Fig. 4A). In

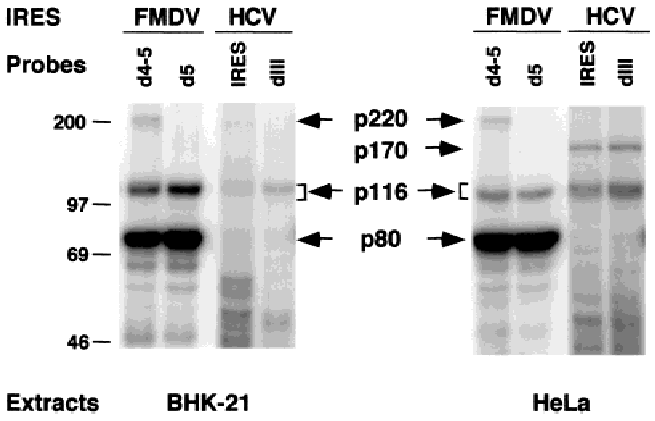

FIGURE 3. Effect of the cytoplasmic extracts from different origin on the RNA–protein interaction pattern of the FMDV IRES. UV-crosslinking pattern obtained for FMDV and HCV IRES RNAs, using S10 extracts from BHK-21 (left) or HeLa cells (right). Crosslinked proteins were resolved in a 8% SDS-PAGE. Molecular weight markers and crosslinked proteins are indicated.

agreement with this observation, the electrophoretic pattern of p116 (Meyer et al., 1982) was resolved later in two polypeptides, p116 and p110 (Asano et al., 1997; Méthod et al., 1997).

As shown in Figure 4B, immunoprecipitation of the crosslinked proteins with an anti-eIF3 serum (Meyer et al., 1982) revealed that two polypeptides with a mobility around 116 kDa interacted with RNA from both FMDV and HCV IRESs. Whereas p110 interacted preferentially with FMDV RNA, p116 seemed to bind more strongly to HCV dIII RNA than to d5 FMDV transcript. A weak p170 crosslinking to the 3′ end of FMDV IRES (Fig. 4A) was also detected after immunoprecipitation with anti-eIF3 serum (Fig. 4B). The p170 subunit of eIF3 immunoprecipitated bound to dIII HCV IRES, consistent with previous reports (Buratti et al., 1998; Sizova et al., 1998). We could also detect small amounts of p80 crosslinked to d5 in the immunoprecipitates, suggesting that the FMDV IRES associated to eIF3 also interacts with eIF4B.

Western blot analysis performed in parallel to the UV-crosslinking assay resulted in the recognition of p116 (Fig. 4C). The serum reacted with p116 from HeLa cells stronger than with the one present in BHK-21 cells. Although this serum contains specific antibodies against most of the eIF3 polypeptides using purified eIF3 preparations (Milburn et al., 1990a), a pattern of lower complexity was observed using this serum with crude HeLa cell extracts (Meyer et al., 1982). Proteins with a molecular mass of 220, 170, and 70–45 kDa were apparent in overexposed films (data not shown). These results allow us to conclude that the protein of 110/116 kDa interacting preferentially with domain 5 of the FMDV IRES is a component of eIF3.

eIF4B binds to domain 5 in the FMDV IRES, but this interaction is not essential for IRES activity in vivo

Even though eIF4B (p80) was undetectable using probes that contained exclusively domain 4 (Fig. 1C), it remained possible that a weak binding to domain 4 could occur below to the limit of detection of the assay. Therefore, we performed competition assays using unlabeled FMDV transcripts d4 and d5. A clear competition of eIF4B binding to d5 was detected when an excess of unlabeled d5 RNA was used as competitor

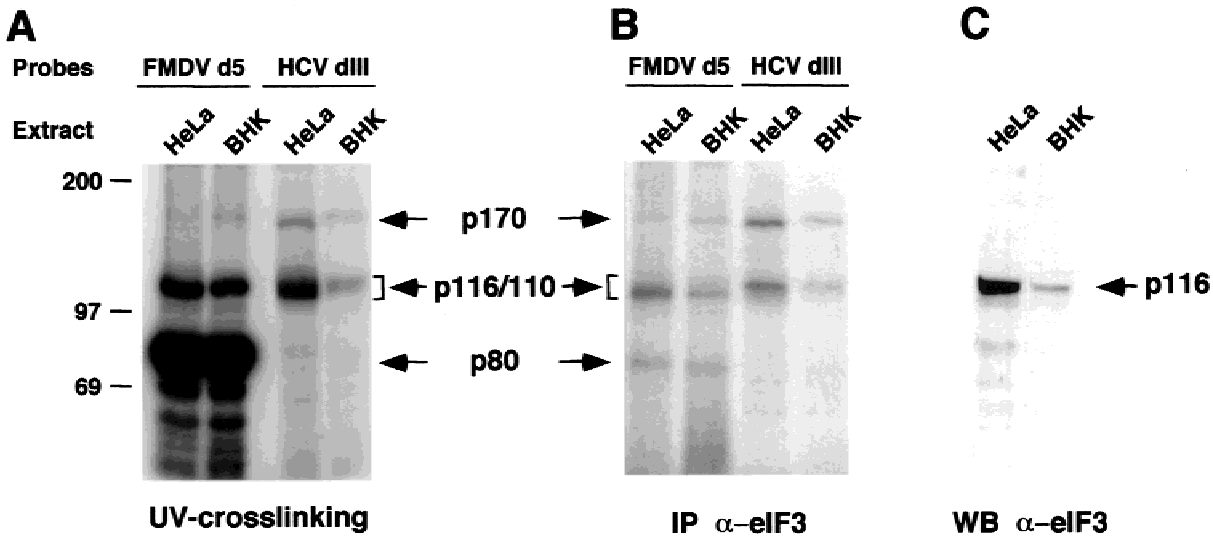

FIGURE 4. Interaction of eIF3 with FMDV IRES. **A:** UV-crosslinking assay performed with d5 of FMDV IRES or with dIII of HCV IRES using S10 extracts from HeLa or BHK-21 cells. Immunoprecipitation (**B**) of crosslinked proteins shown in **A** and western blot analysis (**C**) using a goat anti-eIF3 serum (Meyer et al., 1982). Proteins were resolved in 7% SDS-PAGE.

(Fig. 5A), showing 80% inhibition with 50-fold molar excess (Fig. 5B). In contrast, no significant reduction of the crosslinked eIF4B was apparent for d4 RNA under the same experimental conditions (Fig. 5C), even using a 1,000-fold molar excess of competitor d4 RNA. As a negative control in this titration, we included a large molar excess of HCV dIII (Fig. 5C). Interestingly, HCV dIII competed out the interaction of p116 at about the same molar excess as FMDV d5 did (Fig. 5A,C) but it was unable to titrate out eIF4B interaction, in agreement with the lack of crosslinking to p80 (Fig. 3). We conclude from these data that the specific binding of eIF4B to domain 5 of FMDV IRES does not require sequences present in domain 4.

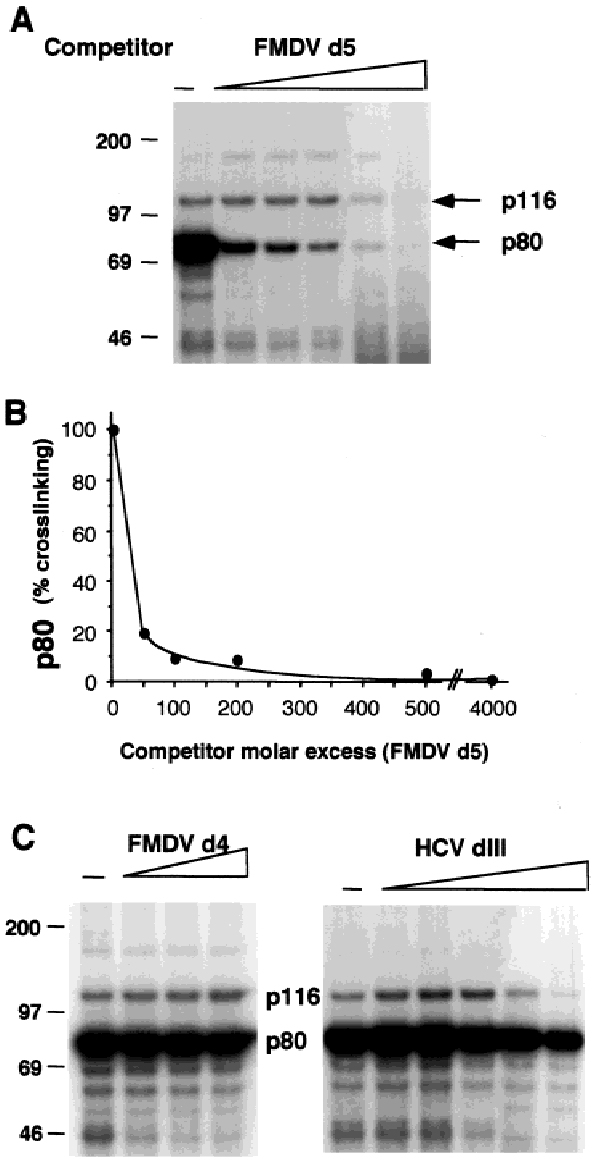

FIGURE 5. Specificity of the eIF4B interaction with the FMDV IRES. **A:** Competition assay with increasing molar excess (0-, 100-, 200-, 1,000-, 2,000-, and 4,000-fold) of unlabeled FMDV d5 to labeled probe (0.025 pmol of d5) in the binding reaction, otherwise performed as in Figure 2A. **B:** The percentage of p80 binding to labeled domain 5 was made relative to the intensity of the crosslinked product in the lane without competitor RNA. **C:** Competition assay of unlabeled FMDV d4 using increasing molar excess (0-, 200-, 500-, and 1,000-fold), or HCV-dIII (0-, 100-, 200-, 1,000-, 2,000-, and 4,000-fold) to labeled probe (0.025 pmol of d5).

Thus domain 5 was necessary and sufficient to mediate eIF4B binding to the FMDV IRES. To investigate the biological relevance of this interaction, we analyzed the genetic variability of domain 5. Whereas the 20-nt region preceding the functional AUG accepts substitutions (Escarmís et al., 1992), the −20 to −44 region is highly conserved among field isolates. Alignment of 24 sequences, representing the seven FMDV serotypes, revealed that 96% of the changes found in the hairpin of domain 5 were compensatory substitutions (Fig. 6A). Moreover the residues located in the internal bulge and the apical loop were conserved whereas the short AAU loop connecting domains 4 and 5 accumulated substitutions (Figs. 1A and 6A). Interestingly, the phylogenetically conserved hairpin of domain 5 resembles the structure found in in vitro selected eIF4B high affinity ligands such as oligo A3 (Fig. 6A; Méthod et al., 1996a).

With the aim of defining the residues in the FMDV IRES involved in eIF4B binding, as well as the requirement of this RNA–protein interaction for in vivo IRES function, we have analyzed the contribution of the internal bulge together with the sequence composition of the apical loop of domain 5 hairpin in (1) the activity of FMDV IRES containing mutations in this stem-loop structure, and (2) the efficiency of eIF4B binding to the mutated IRESs. To this end, we introduced substitutions in the apical loop (positions A_{-33} and G_{-31}; Fig. 6A) that did not modify the predicted secondary structure. Deletion of the internal bulge (A_{-38}) was also performed.

Study of the activity of these IRES mutants in transfected cells, in the context of a bicistronic vector, revealed a mild reduction of activity in vivo relative to the wild type (Fig. 6B). A reduction of two- to fourfold in IRES activity was observed, independently of the mutation introduced in these positions. This is in sharp contrast to mutations disrupting the GNRA motif of domain 3 (López de Quinto & Martínez-Salas, 1997) as well as those affecting the eIF4G binding site in domain 4 (López de Quinto & Martínez-Salas, 2000) that reduced IRES activity by 100 to 1,000-fold. Therefore, the primary sequence of residues in domain 5 of FMDV IRES studied here tolerated substitutions to any other nucleotide without significantly compromising IRES activity in vivo.

To identify the residues involved in eIF4B-IRES interaction, we performed UV-crosslinking assays with two examples of the domain 5 mutants. Surprisingly, a strong reduction in eIF4B binding was observed when these mutants were used as probes in the context of d4-5 (Fig. 6C). To rule out the possibility that eIF4B could have established contacts with the mutant IRES through another RNA region, we studied the eIF4B interaction in the context of the whole IRES. Again, no interaction

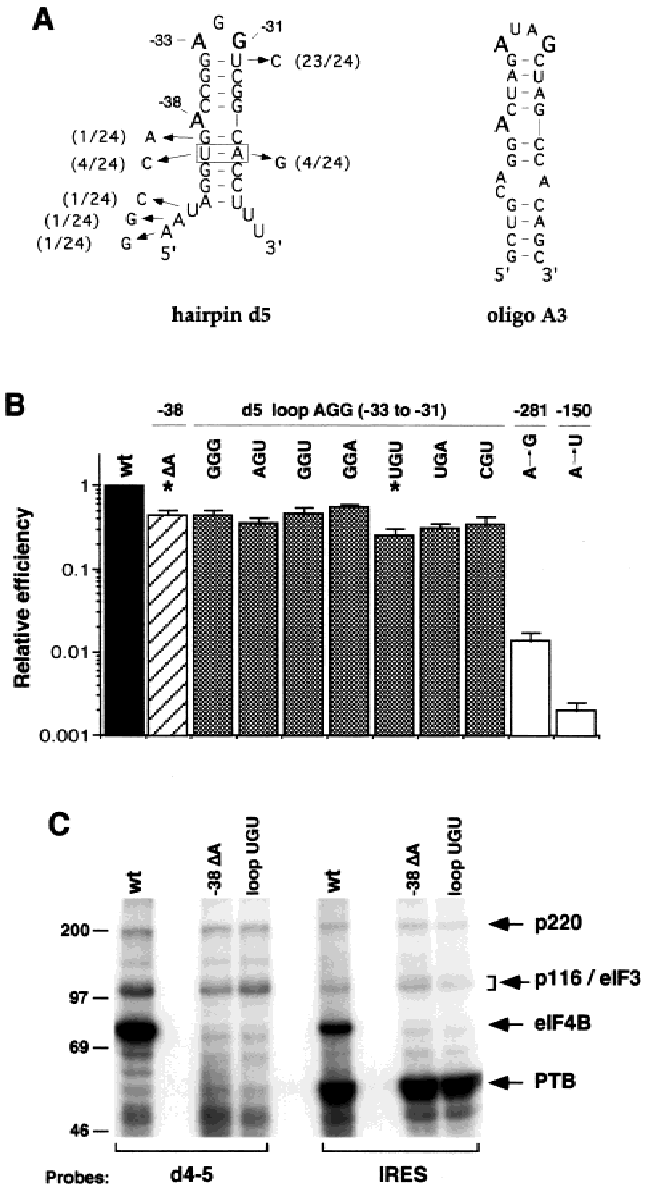

FIGURE 6. Identification of the eIF4B binding site in the FMDV IRES. **A:** Phylogenetic conservation of the sequence of domain 5 in 24 isolates of FMDV. On the right, the consensus sequence found in the in vitro selected eIF4B high affinity ligands (Méthod et al., 1996a). Bold letters denote the residues subjected to site-directed mutagenesis. **B:** Relative IRES activity determined in vivo, in the context of a bicistronic construct, of mutants with the internal bulge (A_{-38}) deleted or single and double substitutions in the apical loop (residues −33 and −31). Mutants −281 (A → G) in the GNRA motif and −150 (A → U) in the internal A loop in domain 4 have been previously described (López de Quinto & Martínez-Salas, 1997, 2000). **C:** Representative domain 5 mutants (shown with asterisks in **B**) were studied in a UV-crosslinking assay, using either d4-5 or the full-length IRES as probe. Proteins were resolved in 8% SDS-PAGE.

of the protein was detected (Fig. 6C), confirming that eIF4B interacts solely with domain 5 and that this binding was lost in the mutants studied. A similar behavior concerning the specificity of eIF4B interaction with high affinity ligands selected in vitro has been described (Méthod et al., 1996a). Altogether, the above results indicated that the internal bulge (A_{-38}) and the nucleotides in the apical loop of domain 5 of FMDV IRES (A_{-33}; G_{-31}) are critical for mediating the binding of eIF4B to the IRES, but this interaction is not essential for in vivo IRES activity.

Interaction of eIF4GII with the FMDV IRES: The Lb protease generates a C-terminal fragment that binds efficiently to the IRES

Little information is so far available concerning the requirement of eIF4GII for internal translation initiation. As eIF4GI and eIF4GII from HeLa cell extracts migrated similarly in SDS-PAGE, with an apparent molecular mass of 220 kDa (Gradi et al., 1998a), we reasoned that the p220 species crosslinked to domain 4 of FMDV IRES could comprise both eIF4GII and the previously identified eIF4GI (López de Quinto & Martínez-Salas, 2000). To check this hypothesis, an immunological characterization of crosslinked p220 was performed using a serum raised against the C-terminal region of eIF4GII. This antibody specifically recognizes the intact protein in HeLa cells, as well as its C-terminal fragment that appears after poliovirus 2A protease cleavage (Goldstaub et al., 2000).

Crosslinking assays were performed with d4-5 as probe and S10 extracts from BHK-21 and HeLa cells, with or without expression of the FMDV Lb protease (Fig. 7A). Interestingly, processing of p220 by Lb led to the appearance of a new crosslinked band with an apparent mobility of 110 and 102 kDa in BHK-21 and HeLa cells, respectively. Immunoprecipitation of the UV-crosslinked proteins with the anti-eIF4GII serum resulted in the recognition of two polypeptides in BHK-21 cell extracts, p220 and p110. As shown in Figure 7B, p220 was apparent in extracts unprocessed by the Lb protease, whereas p110 immunoprecipitated only in Lb-processed extracts, concomitantly with p220 removal. A similar immunoprecipitation pattern was observed with HeLa cell extracts, with the difference that the molecular mass of the proteolytic product was 102 kDa (Fig. 7B). The western blot obtained for HeLa cells transfected with pLb plasmid revealed the presence of signals in p220 and p102 (Fig. 7C), consistent with the immunoprecipitation pattern. Immunoblotting of the BHK-21 crosslinked proteins revealed that the eIF4GII antibody recognized weakly the C-terminal fragment resulting from eIF4GII cleavage by Lb protease although it did not recognize p220.

When domain 4 alone was used as probe, p220 and p116 but not p80 appeared crosslinked both in BHK-21 and HeLa cell extracts (Fig. 7D), as expected from the preferential binding of eIF4B to domain 5. On the other hand, a polypeptide of about 110 kDa appeared in the extracts processed by the Lb protease concomitantly with p220 cleavage. The immunoprecipitation pattern of the crosslinked polypeptides with the anti-eIF4GII

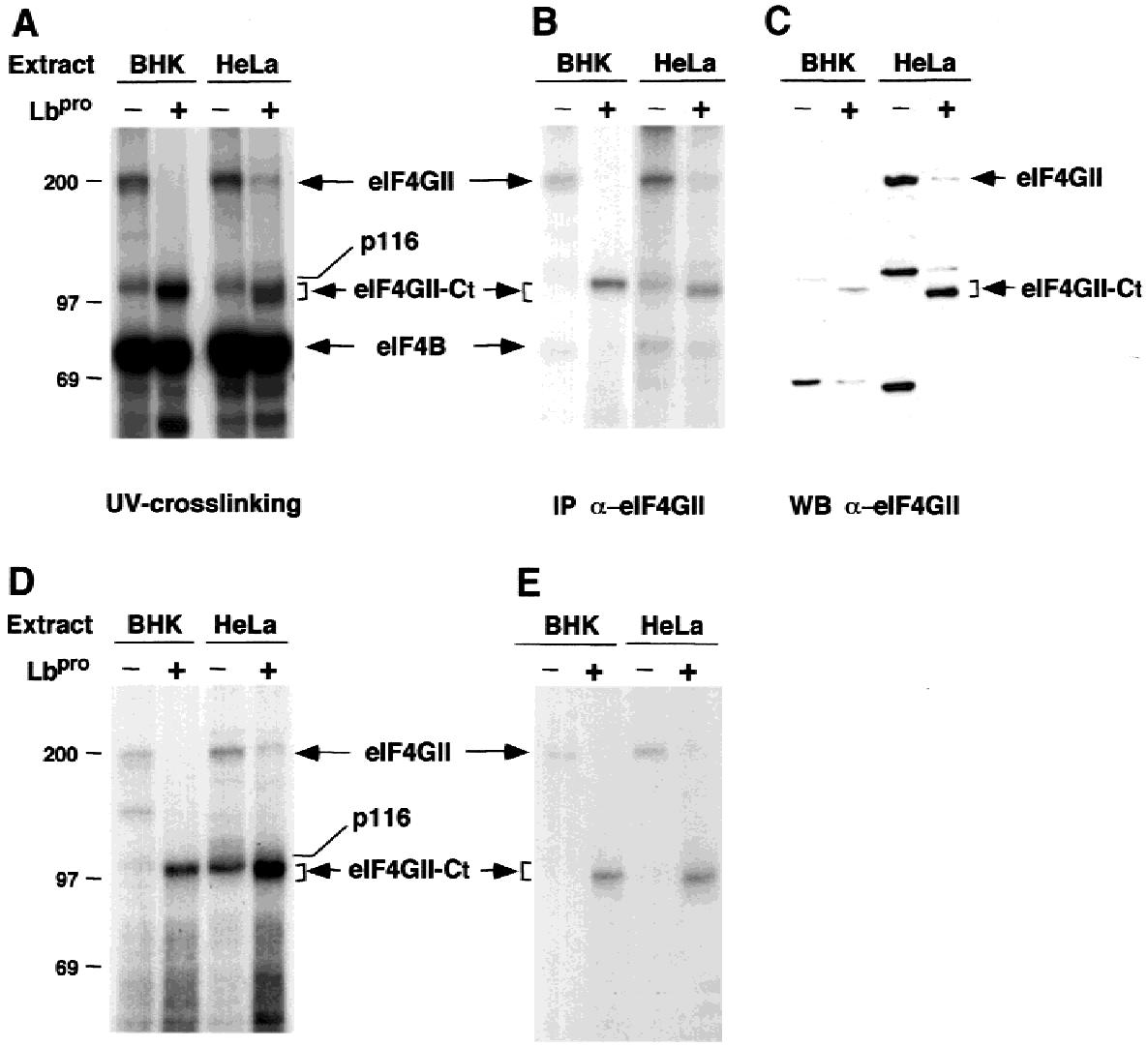

FIGURE 7. Interaction of eIF4GII with the FMDV IRES. **A:** UV-crosslinking assay performed with d4-5 as probe and S10 extracts from BHK-21 and HeLa cells, transfected (+) or not (−) with a plasmid that expresses the FMDV Lb protease. Immunological characterization of crosslinked complexes shown in **A** using an anti-eIF4GII polyclonal serum (Goldstaub et al., 2000), by immunoprecipitation (**B**) and western blot analysis (**C**). **D:** UV-crosslinking assay performed with d4 alone as probe and S10 extracts from BHK-21 and HeLa cells, transfected (+) or not (−) with the pLb plasmid. **E:** anti-eIF4GII immunoprecipitation of the d4-crosslinked products. Proteins were resolved in 7% SDS-PAGE.

serum obtained using d4 alone as probe revealed the appearance of the intact or the Lb-processed eIF4GII protein (Fig. 7E) consistent with results shown in Figure 7B. Taken together, these results demonstrate that eIF4GII interacted exclusively with domain 4 of the FMDV IRES through its C-terminal fragment, generated by the Lb protease cleavage.

Therefore, the p220 crosslinked to the IRES contains both forms of eIF4G, confirming previous data from our laboratory (López de Quinto & Martínez-Salas, 2000). While this work was in progress, the central region of eIFGII was shown to be necessary for in vitro EMCV IRES-dependent 48S complex formation (Marcotrigiano et al., 2001). Substitution of the adenines present in a conserved internal loop at the base of domain 4 of FMDV IRES resulted in the loss of in vivo IRES activity concomitantly with the absence of p220 interaction (López de Quinto & Martínez-Salas, 2000). The lack of p220 interaction in these mutants suggests that both, eIF4GI and eIf4GII, recognize similar RNA determinants in the FMDV IRES.

DISCUSSION

eIF3 initiation factor interacts at multiple sites with the FMDV IRES

We have identified a novel RNA–protein interaction between eIF3 and the FMDV IRES as evidenced by the specific recognition of the IRES-crosslinked p116/110

in immunoprecipitation and western blot by an anti-eIF3 serum. p116 crosslinked to FMDV IRES migrated closely to a protein interacting with HCV IRES. In agreement with the description of a doublet of 116 and 110 kDa in HeLa eIF3 (Asano et al., 1997; Méthod et al., 1997) the crosslinked product consisted of two polypeptides. Remarkably, the p110 subunit, rather than p116, seems to interact preferentially with domain 5 of FMDV IRES (Fig. 4) as opposed to the HCV IRES. A protein of 120 kDa that forms part of eIF3 has been also shown to interact with CSFV and HCV IRES (Buratti et al., 1998; Pestova et al., 1998b; Sizova et al., 1998). Under our conditions, we did not detect eIF4G or eIF4B interaction with HCV IRES (Fig. 3), a result consistent with the observation that 48S complex formation on the HCV IRES requires only eIF3 and the 40S subunit (Pestova et al., 1998b).

It appears that eIF3 contacts with the FMDV IRES at multiple sites. A preferential eIF3 binding site resided in domain 5. However domain 4 also interacted with this factor (Fig. 1C) and, although to a lower extent, we observed crosslink of p116 to domains 1–2 and 3 (Fig. 2). Moreover, we also detected a weak binding of p170, which was recognized by the anti-eIF3 serum (Fig. 4B) suggesting that it could be another eIF3 protein interacting with the FMDV IRES. Under the experimental conditions used here, p170 crosslinking to the FMDV IRES was only detected with probe d5. On the other hand, a weak crosslinked product of about 150 kDa that may correspond to a breakdown product of p170 (Milburn et al., 1990a) was observed in the whole IRES or domain 4–5 probes. By contrast, the HCV IRES interacted with p170 more strongly, either as dIII or the whole IRES (Fig. 3). Definition of other eIF3 subunits mediating binding to IRESs could be of special interest, as some of these proteins seem to be important targets for translation regulation (Guo et al., 2000).

Structural determinants of eIF3-IRES interaction have been found in the central helix of HCV domain III (Odreman-Macchioli et al., 2000; Kieft et al., 2001). However, changes of a few nucleotides in loop IIIa did not significantly affect eIF3 binding or IRES activity, indicating that eIF3-IRES interaction tolerates substitutions in the RNA-binding site that preserve the overall secondary structure (Kolupaeva et al., 2000). The sequence of conserved residues in domains 4 and 5 is not an essential determinant for eIF3 interaction with FMDV IRES (Table 1). It remains to be studied whether destabilization of the domain 5 structure impairs eIF3 binding to the FMDV IRES and concomitantly, affects IRES activity.

Functional implications of eIF4B interaction with FMDV IRES

We have demonstrated that the eIF4B binding site in the FMDV IRES is located in domain 5. Sequence determinants for eIF4B-IRES interaction involved the internal bulge A_{-38} and the A_{-33} and G_{-31} in the apical loop. Mutations introduced in these positions abolished eIF4B binding to FMDV IRES. However, a mild reduction of IRES activity in vivo was observed as compared to the reduction induced by mutations in the binding site of eIF4G (Table 1). Our findings for eIF4B function in vivo during internal initiation of translation are in agreement with the function of eIF4B as a factor capable of stimulating two- to fourfold cap-dependent translation (Pestova et al., 1998a). Accordingly, yeast lacking eIF4B are viable although they grow more slowly (Altmann et al., 1993; Coppolecchia et al., 1993). Therefore, we conclude that eIF4B binding to FMDV IRES RNA is not essential for IRES function in vivo as well as that the apical loop of domain 5 accepts nucleotide changes without compromising strongly IRES activity.

eIF4B contains an RNA recognition motif (RRM) near the N-terminus (Milburn et al., 1990b) and a second RNA-binding region in the carboxy-terminal half of the protein (Méthod et al., 1994; Naranda et al., 1994).

TABLE 1. Relationship between RNA–protein interaction and in vivo IRES activity.

	IRES sequence		Reduction of IRES activity	IRES-protein binding			
	Domain 4	Domain 5		4B p80	eIF3 p116	4GI+4GII p220	PTB p57
	−153 −150	−38 −33 −31					
wt	G C U A A	A C C G G A G G	1	+	+	+	+
−38 ΔA	· · · · ·	Δ · · · · · · ·	2	−	+	+	+
Loop UGU	· · · · ·	· · · · · U · U	4	−	+	+	+
−150 (A → U)	· · · U ·	· · · · · · · ·	500*	+	+	−*	+
−150 (AA → GG)	· · · G G	· · · · · · · ·	1000*	+	+	−*	+

The IRES sequence shows only the differences with that of the wild-type IRES. Nucleotide numbers in the studied residues of domains 4 and 5 are relative to the A in the first functional AUG (López de Quinto & Martínez-Salas, 1999).

Reduction of IRES activity was calculated as the luciferase activity normalized to CAT activity obtained in BHK-21 transfected cells, relative to that of the wild-type IRES, which was set at 1.

The symbols + and − in IRES-protein binding illustrates the modification in the intensity of the UV-crosslinking capacity of the corresponding IRES sequence with the indicated proteins.

*Mutants −150 (A → U) and (AA → GG) were described in López de Quinto and Martínez-Salas (2000).

Although the carboxy-terminal region binds RNA nonspecifically with high affinity, the RRM binds such RNAs inefficiently. RNA-binding specificity of the eIF4B RRM has been studied using in vitro selection with random sequences. The high affinity ligands showed a conserved set of nucleotides located in a structural motif consisting of a bulge stem-loop (Méthod et al., 1996a). Comparison of the oligo A3 ligand to FMDV domain 5 revealed a secondary structure conservation (Fig. 6A). In common to mutations in domain 5 studied here, deletion of the internal bulge or substitutions in the apical loop led to the loss of the RNA-binding capacity of eIF4B to Oligo A3 ligand (Méthod et al., 1996a). These results suggest that eIF4B recognizes its specific target in the FMDV IRES through its RRM domain. To our knowledge, this is the first report describing specific sequences of the eIF4B binding site in a natural mRNA.

The results shown here do not rule out the possibility that eIF4B could exert its function in the internal initiation mechanism through interactions with other components of the translation machinery. In this regard, binding of eIF4B to 18S rRNA (Méthod et al., 1996a) as well as to eIF3 (Méthod et al., 1996b) has been described. It is noteworthy that in the immunoprecipitation performed using crosslinked proteins to the FMDV IRES and specific antibodies for eIF4GI (López de Quinto & Martínez-Salas, 2000), eIF4GII, and eIF3, we observed an enrichment of the specific polypeptide recognized by the serum together with remnants of the other translation factors (Figs. 4B, 7B). This suggests that these proteins could be interacting with the IRES in the form of a ribonucleoprotein complex.

Interaction of eIF4GII with the FMDV IRES occurs at the same site as eIF4GI

We show here the interaction of the initiation factor eIF4GII with the FMDV IRES demonstrating that the p220 crosslinked to domain 4 is composed of eIF4GI and eIF4GII. We have mapped the binding site of eIF4GI to a conserved motif present in the base of domain 4 of FMDV IRES, where the adenines corresponding to the internal loop determine both the eIF4GI binding to the IRES and its activity in vivo (López de Quinto & Martínez-Salas, 2000). Interestingly, no p220 was detected crosslinked to the IRES mutants altered in the base of domain 4, indicating that eIF4GII interaction, which was immunoprecipitated crosslinked to the wild-type domain 4 (Fig. 7D,E), was also lost in the inactive mutants. This result suggests that eIF4GII interaction may also be functionally involved in FMDV IRES activity. Additionally, the lack of binding of eIF4G in the inactive IRES mutants indicates that both proteins, eIF4GI and eIF4GII, have similar sequence determinants for RNA recognition. These results are consistent with the recent description of the eIF4G domain involved in EMCV-IRES interaction (Marcotrigiano et al., 2001) that shows conservation of the critical residues in the central region of the eIF4GI and eIF4GII.

This report provides the first experimental evidence describing eIF4GII cleavage by the FMDV Lb protease. The eIF4GII-crosslinking pattern obtained in BHK-21 cell extracts is similar to the one reported for eIF4GI (López de Quinto & Martínez-Salas, 2000). Both proteins were processed after expression of Lb protease, and both C-terminal fragments presented a similar apparent mobility of 110 kDa. Immunoprecipitation of HeLa cell polypeptides crosslinked to the 3′ end of FMDV IRES using a specific eIF4GI antibody (Aragón et al., 2000) resulted in the specific recognition of a 102-kDa protein, together with the unprocessed p220 (data not shown). These results indicate that the differences found between HeLa and BHK-21 cells concerning cleavage of p220 by Lb and the mobility of its C-terminal fragment are not related with the eIF4G version studied, but with the different amino acid sequence of these proteins in both cell types.

Although the cleavage site of eIF4GII by Lb has not been mapped yet, comparison of its amino acid sequence with that described for eIF4GI (Kirchweger et al., 1994) indicates a partial sequence conservation in the putative Lb cleavage site (ANLG*RT in eIF4GI and ADFG*RQ in eIF4GII). Assuming that Lb protease recognizes this sequence in eIF4GII, similar functional domains would exist after Lb processing in the cleaved eIF4GI and eIF4GII. These fragments would include the eIF3 and eIF4A binding sites (Lamphear et al., 1995; Gradi et al., 1998a). Cleavage of eIF4GII during poliovirus and rhinovirus infections was coincident with the shut-off of cellular protein synthesis (Gradi et al., 1998b; Svitkin et al., 1999). The potential correlation between eIF4GII degradation in FMDV-infected cells and cap-dependent shut-off is currently under study.

eIF4G-IRES interaction is the limiting factor to titrate the IRES. Relative to eIF4G, titration of eIF4B and p110/116 crosslink to the FMDV IRES required a large excess of competitor. Whereas eIF4G-IRES interaction was fully competed out with 40-fold molar excess of competitor RNA (López de Quinto & Martínez-Salas, 2000), eIF4B binding was reduced to 20% at 40-fold molar excess (Fig. 5B). In contrast, 50% inhibition of p116 crosslink was observed at a molar excess above 1,000-fold, regardless of whether the competitor was d5 of FMDV or dIII of HCV (Fig. 5A,C). These results are likely the consequence of differences in both the nature of the interactions that these proteins establish with their RNA target and in their cytoplasmic concentration. Whereas eIF4G and eIF4B concentration is estimated at about 0.5 molecules per ribosome, the levels of some eIF3 polypeptides exceed the molar level of ribosomes (Duncan & Hershey, 1983) and the bulk of the factor remains in the postribosomal fraction (Mengod & Trachsel, 1985).

Relationship between RNA–protein interactions and in vivo FMDV IRES activity

Comparison of IRES activity of mutants in domains 4 and 5 in transfected cells, regarding their capacity to interact with cellular proteins, showed a direct correlation between RNA–protein interaction and in vivo IRES activity only in the case of eIF4G-IRES interaction (Table 1). The crosslinking pattern of domain 5 mutants was identical to the one observed for the wild-type IRES other than their lack of eIF4B interaction (Fig. 6C). On the contrary, domain 4 mutants showed a strong inhibition of IRES activity concomitantly with the absence of eIF4GI and eIF4GII interactions (Table 1). Preservation of RNA–protein interactions other than eIF4G was observed in the context of the whole IRES for PTB (p57), and domain 4–5 for p116/110 (eIF3) and eIF4B (Table 1). Although we could not exclude the possibility that, in addition to eIF4G, other factors that fail to crosslink to the FMDV IRES may participate in the inactivity of domain 4 mutants, our results indicated that the interaction between FMDV IRES and eIF4G is absolutely necessary for internal initiation in vivo, whereas eIF4B-IRES interaction is dispensable for IRES activity under the experimental conditions used in these assays.

The FMDV IRES establish long-range RNA–RNA interactions between structural domains (Ramos & Martínez-Salas, 1999) in a dynamic tertiary structure which is able to mediate multiple contacts with the translational machinery (López de Quinto & Martínez-Salas, 2000; Pilipenko et al., 2000; this report). Interactions between the IRES and some eIFs are essential for IRES activity, as in the case of eIF4GI and eIF4GII. Furthermore, the multiple contacts that the FMDV IRES can establish with the translational machinery, as happens with eIF4B and eIF3, could account for the high expression levels found for the FMDV IRES relative to other elements in a broad range of cell lines (Borman et al., 1997), making this IRES one of the most competitive elements in directing internal translation initiation.

MATERIALS AND METHODS

Plasmid construction

Constructs encoding the FMDV C-S8c1 IRES are schematically represented in Figure 1B. Plasmid d4-5 has been described (Ramos & Martínez-Salas, 1999). Construct d5 was obtained after digestion of d4-5 with *Eco*RI and *Bst*EII, treatment with Klenow and religation. Deletion of the single-stranded region of domain 5 was performed by PCR using the forward primer T7, the reverse primer DelY (CATTAAT TGTAAAGGATCCGTGCCGTG) bearing a *Bam*HI restriction site, and template d4-5. Digestion of the PCR product with *Eco*RI plus *Bam*HI and ligation in d4-5 plasmid treated with the same enzymes yielded d4-5Δss construct. Deletion of domain 4 in this plasmid via *Eco*RI plus *Bst*EII generated the construct containing exclusively the hairpin of domain 5. Constructs named d4-ss and ss were obtained inserting a *Hpa*I site at the end of domain 5 hairpin using a PCR approach (Martínez-Salas et al., 1996). Briefly, the PCR product obtained with primers Dom5-*Hpa*I (GACCGGAGGTGTTAAC CTTTCC) and SP6, was used as a megaprimer in a second PCR with T7 oligonucleotide. The final PCR product was digested with *Eco*RI plus *Bam*HI enzymes and ligated in d4-5 plasmid. Religation of the blunt-end fragment obtained after *Eco*RI and *Hpa*I digestion led to the construct bearing exclusively the single-stranded region, including the polypyrimidine tract (ss probe). The same procedure but using *Hpa*I and *Bst*EII enzymes yielded d4-ss, which lacks the hairpin of domain 5.

The IRES region present in pBIC plasmid (Martínez-Salas et al., 1993) was subjected to site-directed mutagenesis to introduce substitutions in domain 5 hairpin. Mutagenic primers Del-A (AATAGGTGCCGGAGGTCGGC) and dom5-L (AA TAGGTGACCGGNGNTCGGCACC) where used in combination with external primers pBIC-s and pBIC-as (López de Quinto & Martínez-Salas, 2000). Domain 5 mutants chosen for RNA–protein interaction studies were subcloned in the context of d4-5 as described (Ramos & Martínez-Salas, 1999). Additionally, monocistronic versions of domain 5 mutants were generated by *Pst*I digestion of the bicistronic vectors, resulting in the deletion of the CAT gene, placing the IRES sequence next to the T7 promoter. The sequence of the entire length of the IRES under study was obtained using automatic sequencing (ABI PRIM dye terminator cycle sequencing ready reaction kit, Perkin Elmer).

Genotype 1b HCV IRES, spanning nt 40 to 408 of the viral RNA, was cloned in a pGEM3 vector. The large stem-loop structure characteristic of HCV IRES domain III, spanning nt 134 to 290 (Sáiz et al., 1999), was also subcloned in this vector. The resulting HCV dIII construct allows the synthesis of an RNA that contains loops IIIa, IIIb, IIIc, and IIId. Details of the construction of the plasmids containing HCV IRES sequences will be described elsewhere (E. Lafuente & E. Martínez-Salas, in prep.).

In vitro transcription

Prior to in vitro transcription, monocistronic vectors containing the whole IRES sequence mutated in domain 5 and plasmids bearing FMDV IRES regions corresponding to d4-5, d5, d4-ss, and ss were linearized with *Xho*I. Plasmids d4-5Δss and hairpin were digested with *Bam*HI. To generate domain 4 transcript (d4), construct d4-5 was linearized with *Bst*EII. pGEM3 vectors containing the HCV IRES or domain III of the HCV IRES were digested with *Hin*dIII. Linearized DNAs were phenol extracted and ethanol precipitated prior to transcription at 37 °C during 1 h of incubation with 50 U of T7 RNA polymerase (New England Biolabs) in the presence of 0.5–1 μg of linearized template, 50 mM DTT, 0.5 mM each rNTP, and 20 U RNasin (Promega). Transcripts were uniformly labeled to a specific activity of $\sim 10^7$ cpm/pmol using (α^{32}P)-CTP (400 Ci/mmol). Template DNA was digested with 1 U of RQ1 DNase (Promega) and unincorporated (α^{32}P)-CTP eliminated by exclusion chromatography in TE-equilibrated columns. RNA was extracted with phenol-chloroform, ethanol precipitated, and resuspended in TE to a concentration of

0.04 pmol/μL ($\sim 5 \times 10^5$ cpm/μL). RNA integrity was examined by electrophoresis in 6% acrylamide/7 M urea denaturing gels.

S10 cell extracts preparation

BHK-21 and HeLa cells were grown to 100% confluence in 10-cm dishes in 5% calf serum-supplemented DMEM, washed twice with cold PBS, scraped, collected by centrifugation, and processed as described (Gamarnik & Andino, 1997). To obtain S10 cell extracts in which eIF4G was proteolytically processed, BHK-21 and HeLa monolayers were transfected with pLb plasmid (López de Quinto & Martínez-Salas, 2000). Cells were collected 12–16 h posttransfection. Following elimination of cellular debris, the extract was incubated at room temperature for 5–10 min to allow Lb protease cleavage of eIF4G present in untransfected cells. Total protein concentration was measured by the Bradford assay.

UV-crosslinking assays

Uniformly radiolabeled probes (0.04 pmol, $\sim 5 \times 10^5$ cpm) were incubated with S10 cell extract (40–50 μg protein). Binding reactions were carried out in a final volume of 16 μL in the presence of 10 mM HEPES-KOH, pH 7.4, 35 mM KCl, 2.75 mM $MgCl_2$, 10% glycerol, 0.05% NP40, 0.5 mM DTT, 1 μg/μL yeast tRNA. Reactions were incubated 15–20 min at room temperature and exposed to UV light (254 nm, Stratalinker 1800, Stratagene) 30 min on ice, at a distance of 10 cm from the lamp. In competition assays, unlabeled RNA was added to the binding mixture prior to the probe (0.025 pmol) and incubated 3 min at room temperature. After digestion of the nonprotected probe with 0.3 μg/μL of RNase A during 40 min at 37 °C, loading buffer was added to the samples, boiled for 2 min, and then resolved in SDS-PAGE. ^{32}P-labeled proteins were visualized by autoradiography of the dried gels. Intensity of the crosslinked products was measured in a Phosphorimager. In each case, UV-crosslinking assays were repeated at least three times.

Immunoprecipitation and western blot

Immunoprecipitation of crosslinked complexes was performed essentially as described (López de Quinto & Martínez-Salas, 2000). Briefly, 32 μL UV-crosslinked complexes were diluted with 30 μL of PBS and 50 μL of RIPA (50 mM Tris-HCl, pH 7.5, 150 mM NaCl, 1% Triton X-100, 0.1% SDS, 1% Na-DOC) and incubated with complexes of the corresponding serum with protein A-Sepharose or protein G-agarose (Sigma), during 2 h at room temperature. The beads were washed five times with RIPA and once with TBS prior to adding sample buffer, boiling for 2 min, and loading into SDS-PAGE. For western blot assays, proteins were transferred to nitrocellulose membranes (0.2 μm pore) following electrophoresis separation, using a semidry electrotransfer device (BioRad) according to the instructions of the manufacturer. Identification of the RNA-crosslinked proteins was performed with polyclonal antibodies at the following dilutions: α-C_t eIF4GII 1:1,000 (Goldstaub et al., 2000); α-eIF3, 1:2,000 (Meyer et al., 1982). Polyclonal serum specific for the carboxyl end of eIF4GII or eIF3 were kind gifts from N. Sonenberg and J. Hershey, respectively.

In vivo IRES activity

Relative IRES activity was quantified as the expression of luciferase normalized to that of chloramphenicol acetyltransferase from bicistronic mRNAs (López de Quinto & Martínez-Salas, 1998). Transfection of 80–90% confluent BHK-21 monolayers was carried out using cationic liposomes prepared as described (Rose et al., 1991), 1 h after infection with the vaccinia virus recombinant vTF7-3 expressing the T7 RNA polymerase (Fuerst et al., 1986). Extracts from 1–2 $\times 10^5$ cells were prepared 20 h posttransfection in 100 μL of 50 mM Tris-HCl, pH 7.8, 120 mM NaCl, 0.5% NP40. Experiments were performed on triplicate wells and each experiment was repeated at least three times.

ACKNOWLEDGMENTS

We thank Drs. A. Gradi and N. Sonenberg for providing the polyclonal serum against eIF4GII and J. Hershey for goat anti-eIF3 serum, E. Cano for his excellent technical assistance, and Drs. J.M. Sierra and C. Gutiérrez for helpful suggestions on the manuscript. This work was supported by grants PM98.0122 from Direccion General de Enseñanza Superior, 07B/0039/1999 from Comunidad Autónoma de Madrid, and by an Institutional grant from Fundación Ramón Areces.

Received March 22, 2001; returned for revision
April 20, 2001; revised manuscript received
May 25, 2001

REFERENCES

Altmann M, Müller PP, Wittmer B, Ruchti F, Lanker S, Trachsel H. 1993. A *Saccharomyces cerevisiae* homologue of mammalian translation initiation factor 4B contributes to RNA helicase activity. *EMBO J 12*:3997–4003.

Altmann M, Wittmer B, Méthod N, Sonenberg N, Trachsel H. 1995. The *Saccharomyces cerevisiae* translation initiation factor Tif3 and its mammalian homologue eIF-4B have RNA annealing activity. *EMBO J 14*:3820–3827.

Aragón T, de la Luna S, Novoa I, Carrasco L, Ortín J, Nieto A. 2000. Eukaryotic translation initiation factor 4GI is a cellular target for NS1 protein, a translational activator of influenza virus. *Mol Cell Biol 20*:6259–6268.

Asano K, Kinzy TG, Merrick WC, Hershey JWB. 1997. Conservation and diversity of eukaryotic translation initiation factor eIF3. *J Biol Chem 272*:1101–1109.

Belsham GJ, Jackson RJ. 2000. Translation initiation on picornavirus RNA. In: Sonenberg N, Hershey JWB, Mathews MB, eds. *Translational control of gene expression*. Cold Spring Harbor, New York: Cold Spring Harbor Laboratory Press. pp 869–900.

Block KL, Vornlocher HP, Hershey JWB. 1998. Characterization of cDNAs encoding the p44 and p35 subunits of human translation initiation factor eIF3. *J Biol Chem 273*:31901–31908.

Borman AM, Le Mercier P, Girard M, Kean KM. 1997. Comparison of picornaviral IRES-driven internal initiation of translation in cultured cells of different origins. *Nucleic Acids Res 25*:925–932.

Buratti E, Tisminetzky S, Zotti M, Baralle FE. 1998. Functional analysis of the interaction between HCV 5′ UTR and putative subunits of eukaryotic translation initiation factor eIF3. *Nucleic Acids Res 26*:3179–3187.

Carter MS, Kuhn KM, Sarnow P. 2000. Cellular internal ribosome entry site elements and the use of cDNA microarrays in their investigation. In: Sonenberg N, Hershey JWB, Mathews MB, eds.

Translational control of gene expression. Cold Spring Harbor, New York: Cold Spring Harbor Laboratory Press. pp 615–636.
Coppolecchia R, Buser P, Stotz A, Linder P. 1993. A new yeast translation initiation factor suppresses a mutation in the eIF-4A RNA helicase. *EMBO J 12*:4005–4011.
Duncan R, Hershey JWB. 1983. Identification and quantitation of levels of protein synthesis initiation factors in crude HeLa cell lysates by two-dimensional polyacrylamide gel electrophoresis. *J Biol Chem 258*:7228–7235.
Escarmís C, Toja M, Medina M, Domingo E. 1992. Modifications of the 5′ untranslated region of foot-and-mouth disease virus after prolonged persistence in cell cultures. *Virus Res 26*:113–125.
Fuerst TR, Niles EG, Studier FW, Moss B. 1986. Eukaryotic transient-expression system based on recombinant vaccinia virus that synthesizes bacteriophage T7 RNA polymerase. *Proc Natl Acad Sci USA 83*:8122–8126.
Gamarnik AV, Andino R. 1997. Two functional complexes formed by KH domain containing proteins with the 5′ noncoding region of poliovirus RNA. *RNA 3*:882–892.
Gingras AC, Raught B, Sonenberg N. 1999. eIF4 initiation factors: Effectors of mRNA recruitment to ribosomes and regulators of translation. *Annu Rev Biochem 68*:913–963.
Goldstaub D, Gradi A, Bercovitch Z, Grosmann Z, Nophar Y, Luria S, Sonenberg N, Kahana C. 2000. Poliovirus 2A protease induces apoptotic cell death. *Mol Cell Biol 20*:1271–1277.
Gradi A, Imataka H, Svitkin YV, Rom E, Raught B, Morino S, Sonenberg N. 1998a. A novel functional human eukaryotic translation initiation factor 4G. *Mol Cell Biol 18*:334–342.
Gradi A, Svitkin YV, Imataka H, Sonenberg N. 1998b. Proteolysis of human eukaryotic translation initiation factor eIF4GII, but not eIF4GI, coincides with the shutoff of host protein synthesis after poliovirus infection. *Proc Natl Acad Sci USA 95*:11089–11094.
Guo J, Hui DJ, Merrick WC, Sen GC. 2000. A new pathway of translation regulation mediated by eukaryotic initiation factor 3. *EMBO J 19*:6891–6899.
Hershey JWB, Merrick WC. 2000. Pathway and mechanism of initiation of protein synthesis. In: Sonenberg N, Hershey JWB, Mathews MB, eds. *Translational control of gene expression.* Cold Spring Harbor, New York: Cold Spring Harbor Laboratory Press. pp 33–88.
Jang SK, Krausslich HG, Nicklin MJ, Duke GM, Palmenberg AC, Wimmer E. 1988. A segment of the 5′ nontranslated region of encephalomyocarditis virus RNA directs internal entry of ribosomes during in vitro translation. *J Virol 62*:2636–2643.
Kieft JS, Zhou K, Jubin R, Doudna JA. 2001. Mechanism of ribosome recruitment by hepatitis C IRES RNA. *RNA 7*:194–206.
Kirchweger R, Ziegler E, Lamphear BJ, Waters D, Liebig HD, Sommergruber W, Sobrino F, Hohenadl C, Blaas D, Rhoads RE, Skern T. 1994. Foot-and-mouth disease virus leader proteinase: Purification of the Lb form and determination of its cleavage site on eIF-4 gamma. *J Virol 68*:5677–5684.
Kolupaeva VG, Pestova TV, Hellen CUT. 2000. Ribosomal binding to the internal ribosomal entry site of classical swine fever virus. *RNA 6*:1791–1807.
Kolupaeva V, Pestova TV, Hellen CUT, Shatsky IN. 1998. Eukaryotic translation initiation factor 4G recognizes a specific structural element within the internal ribosome entry site of encephalomyocarditis virus RNA. *J Biol Chem 273*:18599–18604.
Lamphear BJ, Kirchweger R, Skern T, Rhoads RE. 1995. Mapping of functional domains in eukaryotic protein synthesis initiation factor 4G (eIF4G) with picornaviral proteases. Implications for cap-dependent and cap-independent translation initiation. *J Biol Chem 270*:21975–21983.
Lomakin IB, Hellen CUT, Pestova TV. 2000. Physical association of eukaryotic initiation factor 4G (eIF4G) with eIF4A strongly enhances binding of eIF4G to the internal ribosomal entry site of encephalomyocarditis virus and is required for internal initiation of translation. *Mol Cell Biol 20*:6019–6029.
López de Quinto S, Martínez-Salas E. 1997. Conserved structural motifs located in distal loops of the aphthovirus internal ribosome entry site domain 3 are required for internal initiation of translation. *J Virol 71*:4171–4175.
López de Quinto S, Martínez-Salas E. 1998. Parameters influencing translational efficiency in aphthovirus IRES-based bicistronic expression vectors. *Gene 217*:51–56.
López de Quinto S, Martínez-Salas E. 1999. Involvement of the aphthovirus RNA region located between the two functional AUGs in start codon selection. *Virology 255*:324–336.
López de Quinto S, Martínez-Salas, E. 2000. Interaction of the eIF4G initiation factor with the aphthovirus IRES is essential for internal initiation of translation in vivo. *RNA 6*:1380–1392.
Luz N, Beck E. 1991. Interaction of a cellular 57-kilodalton protein with the internal translation initiation site of foot-and-mouth disease virus. *J Virol 65*:6486–6494.
Marcotrigiano J, Lomakin IB, Sonenberg N, Pestova TV, Hellen CUT. 2001. A conserved HEAT domain within eIF4G directs assembly of the translation initiation machinery. *Mol Cell 7*:193–203.
Martínez-Salas E, Ramos R, Lafuente E, López de Quinto, S. 2001. Functional interactions in internal translation initiation directed by viral and cellular IRES elements. *J Gen Virol 82*:973–984.
Martínez-Salas E, Regalado MP, Domingo E. 1996. Identification of an essential domain for internal initiation of translation in the aphthovirus IRES, and implications for viral evolution. *J Virol 70*:992–998.
Martínez-Salas E, Sáiz JC, Dávila M, Belsham GJ, Domingo E. 1993. A single nucleotide substitution in the internal ribosome entry site of foot-and-mouth disease virus leads to enhanced cap-independent translation in vivo. *J Virol 67*:3748–3755.
Mengod G, Trachsel H. 1985. Eukaryotic protein synthesis initiation factor eIF-3: Determination of concentration and association with ribosomes in rabbit reticulocyte and HeLa cell lysates. *Biochimica et Biophysica Acta 825*:169–174.
Méthod N, Pause A, Hershey JWB, Sonenberg N. 1994. The translation initiation factor eIF-4B contains an RNA-binding region that is distinct and independent from its ribonucleoprotein consensus sequence. *Mol Cell Biol 14*:2307–2316.
Méthod N, Pichett G, Keene JD, Sonenberg N. 1996a. In vitro RNA selection identifies RNA ligands that specifically bind to eukaryotic translation initiation factor 4B: The role of the RNA recognition motif. *RNA 2*:38–50.
Méthod N, Rom E, Olsen H, Sonenberg N. 1997. The human homologue of the yeast Prt1 protein is an integral part of the eukaryotic initiation factor 3 complex and interacts with p170. *J Biol Chem 272*:1110–1116.
Méthod N, Song MS, Sonenberg N. 1996b. A region rich in aspartic acid, arginine, tyrosine, and glicine (DRYG) mediates eukaryotic initiation factor 4B (eIF4B) self-association and interaction with eIF3. *Mol Cell Biol 16*:5328–5334.
Meyer K, Petersen A, Niepmann M, Beck E. 1995. Interaction of eukaryotic initiation factor eIF-4B with a picornavirus internal translation initiation site. *J Virol 69*:2819–2824.
Meyer LJ, Milburn SC, Hershey JWB. 1982. Immunochemical characterization of mammalian protein synthesis initiation factors. *Biochemistry 21*:4206–4212.
Milburn SC, Duncan RF, Hershey JWB. 1990a. Immunoblot analysis of the structure of protein synthesis initiation factor eIF3 from HeLa cells. *Arch Biochem Biophys 276*:6–11.
Milburn SC, Hershey JWB, Davies MV, Kelleher K, Kaufman RJ. 1990b. Cloning and expression of eukaryotic initiation factor 4B: Sequence determination identifies a common RNA recognition motif. *EMBO J 9*:2783–2790.
Naranda T, Strong WB, Menaya J, Fabbri BJ, Hershey JWB. 1994. Two structural domains of initiation factor eIF-4B are involved in binding to RNA. *J Biol Chem 269*:14465–14472.
Nygard O, Westermann P. 1982. Specific interaction of one subunit of eukaryotic initiation factor eIF-3 with 18S ribosomal RNA within the binary complex, eIF-3-small ribosomal subunit, as shown by cross-linking experiments. *Nucleic Acids Res 10*:1327–1334.
Odreman-Macchioli FE, Tisminetzky SG, Zotti M, Baralle FE, Buratti E. 2000. Influence of correct secondary and tertiary RNA folding on the binding of cellular factors to the HCV IRES. *Nucleic Acids Res 28*:875–885.
Pelletier J, Sonenberg N. 1988. Internal initiation of translation of eukaryotic mRNA directed by a sequence derived from poliovirus RNA. *Nature 334*:320–325.
Pestova TV, Borukhov SI, Hellen CUT. 1998a. Eukaryotic ribosomes require initiation factors 1 and 1A to locate initiation codons. *Nature 394*:854–859.

Pestova TV, Hellen CUT, Shatsky IN. 1996. Canonical eukaryotic initiation factors determine initiation of translation by internal ribosomal entry. *Mol Cell Biol 16*:6859–6869.

Pestova TV, Shatsky IN, Fletcher SP, Jackson RJ, Hellen CUT. 1998b. A prokaryotic-like mode of cytoplasmic eukaryotic ribosome binding to the initiation codon during internal initiation of hepatitis C and classical swine fever virus RNAs. *Genes & Dev 12*:67–83.

Pilipenko EV, Pestova TV, Kolupaeva VG, Khitrina EV, Poperechnaya AN, Agol VI, Hellen CUT. 2000. A cell cycle-dependent protein serves as a template-specific translation initiation factor. *Genes & Dev 14*:2028–2045.

Preiss T, Hentze WM. 1999. From factors to mechanism: Translation and translational control in eukaryotes. *Curr Opin Gen Dev 9*:515–521.

Ramos R, Martínez-Salas, E. 1999. Long-range RNA interactions between structural domains of the aphthovirus internal ribosome entry site (IRES). *RNA 5*:1374–1383.

Rose JK, Buonocore L, Whitt MA. 1991. A new cationic liposome reagent mediating nearly quantitative transfection of animal cells. *Biotechniques 10*:520–525.

Rozen F, Edery I, Meerovitch K, Dever TE, Merrick WC, Sonenberg N. 1990. Bidirectional RNA helicase activity of eukaryotic translation initiation factor 4A and 4F. *Mol Cell Biol 10*:1134–1144.

Sáiz JC, López de Quinto S, Ibarrola N, López-Labrador FX, Sánchez-Tapias JM, Rodés J, Martínez-Salas E. 1999. Internal initiation of translation efficiency in different hepatitis C genotypes isolated from interferon treated patients. *Arch Virol 144*:1–15.

Sizova DV, Kolupaeva VG, Pestova TV, Shatsky IN, Hellen CUT. 1998. Specific interaction of eukaryotic translation initiation factor 3 with the 5′ nontranslated regions of hepatitis C virus and classical swine fever virus RNAs. *J Virol 72*:4775–4782.

Svitkin YV, Gradi A, Imataka H, Morino S, Sonenberg N. 1999. Eukaryotic initiation factor 4GII (eIF4GII), but not eIF4GI, cleavage correlates with inhibition of host cell protein synthesis after human rhinovirus infection. *J Virol 73*:3467–3472.

Tarun SZ Jr, Sachs AB. 1996. Association of the yeast poly(A) tail binding protein with translation initiation factor eIF-4G. *EMBO J 15*:7168–7177.

Wilson JE, Pestova TV, Hellen CUT, Sarnow P. 2000. Initiation of protein synthesis from the A site of the ribosome. *Cell 102*:511–520.